Principles of Anti-Aging Combination Therapies

Principles of Anti-Aging Combination Therapies

By

Anatoly Mayburd

Cambridge
Scholars
Publishing

Principles of Anti-Aging Combination Therapies

By Anatoly Mayburd

This book first published 2024

Cambridge Scholars Publishing

Lady Stephenson Library, Newcastle upon Tyne, NE6 2PA, UK

British Library Cataloguing in Publication Data
A catalogue record for this book is available from the British Library

ISBN (10): 1-0364-0480-3
ISBN (13): 978-1-0364-0480-2

TABLE OF CONTENTS

PREFACE

This book is dedicated to my parents. I wish that everybody enjoyed their loved ones for a bit longer. Showing substantial scientific evidence that a life extension by as many as a few decades is not only desired but feasible is the objective. We make specific proposals for the research on the new frontiers.

Our work keeps as close as possible to the achievements of others and to the experimentally established facts, avoiding unrealistic conclusions. It cites ~ 1000 of the leading reports in the longevity field. This makes bold projections and daring ideas more valuable, knowing that they are not sensational but rather follow the field. This field – like artificial intelligence - naturally leads to futuristic ideas; it promises enormously disruptive and transformative changes in the coming decades, calling for a wide reform of societal priorities, decision-making, and preparedness for the future.

The book is written in a semi-popular style, balancing scientific rigor with availability; it cites key references without encumbering with too much technical detail. Yet it provides enough introduction to each subject to make it amenable to knowledge-seekers of all kinds, including biomedical professionals in search of new proposals and perspectives. In the chapters discussing lifestyle factors and multimodalities, the book provides a quantitative scoring system to estimate potential additions and subtractions to the expected personal lifespan, assessed by epigenetic clocks or other predictors. The book strongly relies on the data from electronic medical records and the computational analysis of the published high-throughput datasets. Such sources appear to be biased but find systematic confirmation in experimental biology and clinical trials. This means the predicted delays in the aging rate due to choices of lifestyle, educational level, attitudes, prescription drugs, and supplements are also real.

The data are consistent with the idea that the aging rate is not a pre-set, inexorable consequence of a person's genotype but, to a great degree, is a choice, even at today’s embryonic level of knowledge. Our work provides multiple ideas for the research of the future, being useful for biomedical

professionals designing new experiments, doctors in search of clinical trial proposals, and students infatuated with this tantalizing field.

CHAPTER 1

ACTUARIAL AND BIOLOGICAL AGING: INTRODUCTION

1. Historical trends in longevity

We start Chapter 1 by paying tribute to past generations and the curiosity, labor, and spiritual focus that led to scientific and technological discovery. It is thanks to the foundation of medicine, improved agriculture, public health and hygiene, food and drug safety control, environmental controls, residential construction norms, health information awareness, detective and police work, and the general absence of political violence in the Western world over the last 70 years that life expectancy has made strides. The trend toward greater life expectancy continues, and in many societies, it is not abating. Figure 1 presents a panoramic view of longevity progress in France between 1816 and 2018.

Figure 1 shows that in 1816, the survival rate of 0.5 was reached at the age of 35; in 1916, the same survival rate was reached at the age of 57; and in 2018, at the age of 85. The survival rate of 0.2 was reached in 1816 at the age of 70, in 1916 at the age of 75, and in 2018 at the age of 93. Over the last 200 years, the shape of the survival curve has become more rectangular. Childhood survival is the greatest gainer, with 20% of the newborns dying within the first year in 1816, 11% in 1916, and 0.36% in 2018. For the 76–80-year bracket, the fraction of survival increased from 44% in 1995 to 64% in 2018, over a period of 23 years, or 0.87% per year. For the previous 20 years (1974–1994), the gain was from 32% to 44%, or 0.6% per year. For the still-prior 20 years (1953–1973), the gain was from 17% to 32%, or 0.75% per year. The increments for the prior historical periods are much smaller, and for this age bracket, the greatest rate of change is occurring now.

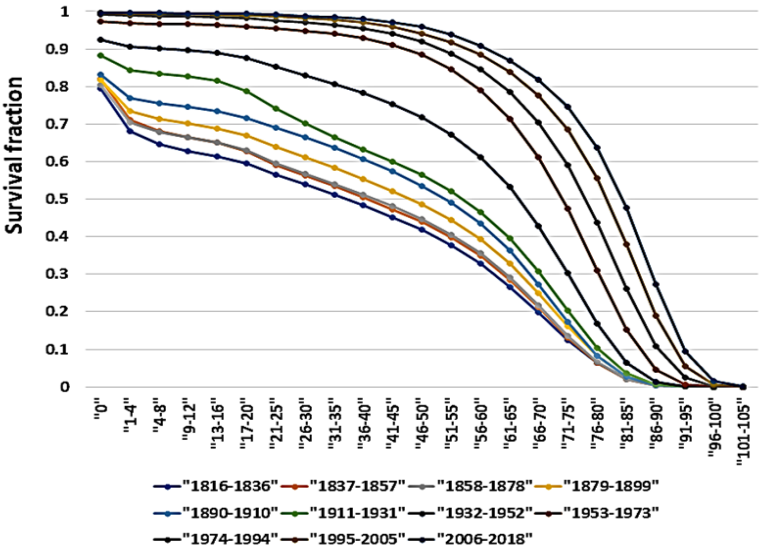

Figure 1: Survival fraction as a function of age and historical period, based on the data of Human Mortality Database (https://www.mortality.org/). The age ranges from "0" (0–1 year) to the "101–105" bracket. The historical periods are intervals of 20 years starting with 1816 shown below the abscissa. The last two intervals (1995–2005, 2006–2018) are 10 and 12 years, respectively. The upper curves are more recent. The survival curve was computed by relating all mortality in the historical interval to all population numbers in the given age bracket. Survival past the age bracket is:

$$S(T) = S(T) \times (1 - M(T))^N \quad (1)$$

Where S(T) is the survival fraction past the age bracket, S(T') is the survival fraction prior to the age bracket, M(T) is the average mortality in the age bracket, and N is the number of years in the age bracket.

2. Does human longevity demonstrate the upper limit?

Does a limit on human longevity exist? In the data in Figure 1, the fraction of individuals older than 90 moved from 0.6% in 1816 to... 0.6% in 1916, and then to a whopping 28% in 2018. Figure 2A shows the fraction of nonagenarians, centenarians, and super-centenarians in the French population between 1816 and 2018, while Figure 2B validates it with the all-cause mortality rates.

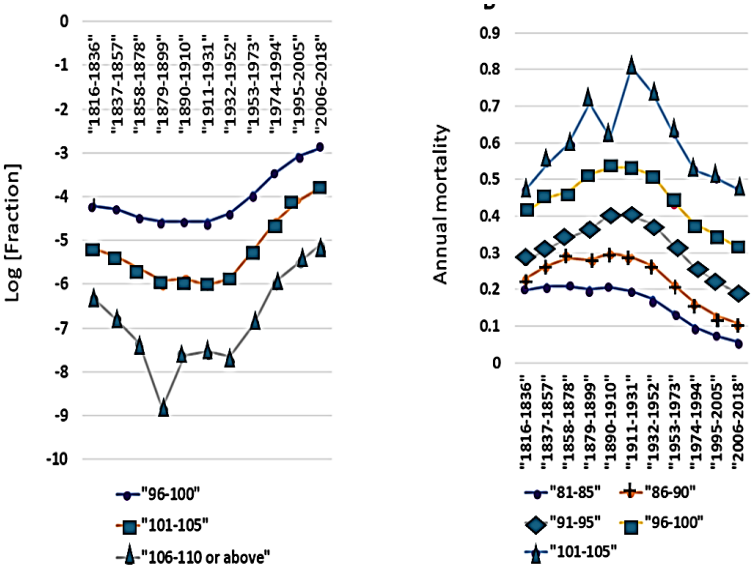

Figure 2: The log fractions of the oldest old age strata in the French population between 1816 and 2018 (Figure 2A) and the annual mortality rates for the different age brackets in the period between 1816 and 2018 (Figure 2B). In Figure 2A, "96-100" is the upper curve. In Figure 2B, "101-105" is the upper curve.

The fraction of the oldest old passed a minimum in French society *in the most stressful period of the late 19th and first half of the 20th century, before 1952*. The fraction data is confirmed by the mortality, showing a reciprocal trend. *The mortality rates for the 81–85-years brackets did not decline between 1816 and 1931, while the mortality rates for the older strata increased over the same period*! After reaching the maximum, the mortality rates began to decline after 1952 for all brackets. *For the 110+ bracket (314 observations for 1816–1836 in France), the mortality rate returned to the level of 1816 only by 2018.* For the 106–110 bracket, the mortality rate declined and reached the 1816 level in the 1960s. While premature mortality rates were declining for the younger ages over 1816–2018, the maximal lifespan was experiencing complex shifts.

Age records available in public data need careful documentation, especially in the 110+ category, where a desire for fame, financial incentives, and ambition may conspire to exaggerate. Younger individuals may be able to pass the safeguards and get longer access to financial benefits by falsifying records. Other sources of uncertainty are the lack of documentation (birth

certificates or church records), poor cognitive status, and unreliable census data. The problems with vital records escalate with age and decreased socio-economic status (see Coale et al., Preston et al., Dechter et al., Gavrilov et al., and Newman et al.). Newman et al. call attention to linking civil registration rates to per-capita estimates of remarkable age attainment in central population registries and validated supercentenarian databases in the USA and Italy.

Remarkable age attainment is predicted by indicators of error and fraud, including illiteracy, poverty, high crime rates, short average lifespans, and the absence of birth certificates. According to Newman et al., the introduction of state-wide birth certification parallels a reduction in the number of supercentenarians. In total, 82% of supercentenarian records from the USA (N=536) predate state-wide birth certification. Forty-two states achieved complete birth certificate coverage during the survey period. When these states reformed birth registration, the number of supercentenarians fell by 80% per year, or approximately 69% per capita. The work of Newman et al. is disputed: there is a residual supercentenarian population after the records are standardized (there is a 69% per-capita drop, but 31% passes validation). Wachter et al. and Barbi et al. collected 4000 validated records using the Italian system of birth registrations in place since 1860. The presence of birth records attached to the reported age rules out "contamination" of the study cohorts by the falsified ages. The mortality rate does display a plateau in the work of Barbi et al., consistent with the stabilization of "death force" or "hazard function" at the extreme ages.

One approach to address uncertainty is the extrapolation of trends existing in the bulk of the population to the extreme edge of longevity. Individuals that misrepresent the "desired" age for the next census *will demonstrate a lower mortality rate than their real peers in the same demographic group*. While the annual attrition rate increases and then stabilizes at some high fraction (0.4–0.8) in individuals after 95, *the inversion of this trend after 110 can be explained by low-quality records*. Not all is so obvious. There is a school of thought that claims a so-called "mortality crossover" among the super-centenarians. The "mortality crossover" theory states that supercentenarians are genetically or phenotypically distinct from the general population and die at a lower rate (see below). One mechanism is selection. A population with higher mortality at younger ages will select the fittest individuals in later life, and they will outlive their peers with lower selective pressure at younger ages (Markides et al.). While the mortality rates are higher in younger blacks, after 74, the blacks outlive the whites, and this effect is noticeable in relatively younger cohorts (Figure 3).

Figure 3 illustrates that the mortality rates are indeed lower over the ages of 1-70 years for non-Hispanic whites, followed by Hispanics, followed by non-Hispanic blacks. However, the curves in Figure 3A visibly cross after

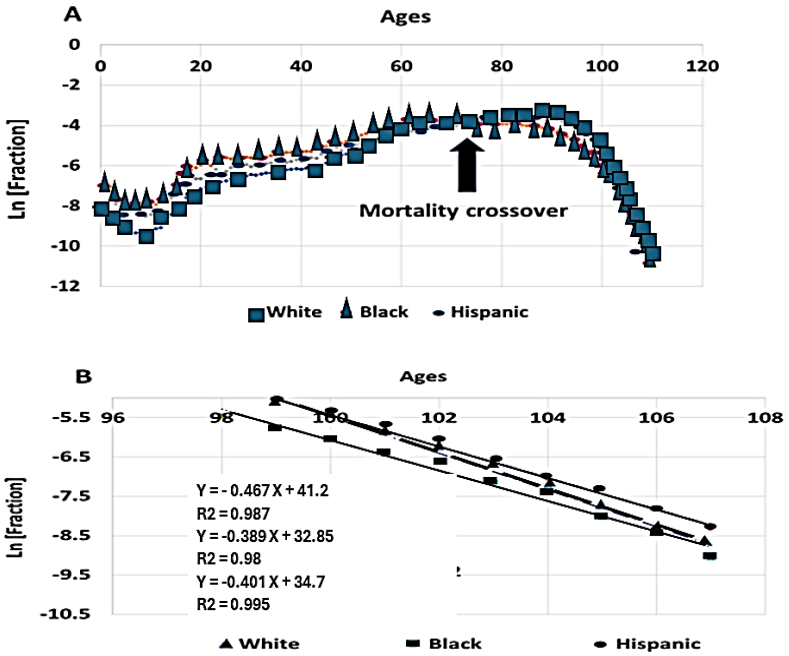

Figure 3: Mortality cross-over effects between non-Hispanic whites, non-Hispanic blacks, and Hispanics in the USA. The data source is the National Bureau of Economic Research (NBER) depository, called "Multiple Causes of Mortality" (https://www.nber.org/research/data/mortality-data-vital-statistics-nchs-multiple-cause-death-data).

The analysis includes the entire range from 1 to 109 years. The decedent data for 2018 was extracted, and the individuals were categorized based on race. In each category, the counts of the decedents of each age were converted into annual fractions of the total. The annual fractions were converted into logarithms to display a wide range of values.

(A) The logarithmic plot of survival fractions ln S or decedent fractions ln D produces a linear segment in the oldest old, and the slope of the segment corresponds to the mortality risk in the given population. The bottom curve to the left of cross-over point are Whites (squares), followed by Hispanics (circles), with the top curve

being Blacks (triangles). Blacks form the bottom curve to the right of the crossover point.

(B) The analysis of the sub-range between 96 and 107 years. The logarithmic fractions form linear plots in this sub-range. The plots are fitted by a linear trendline. The slope coefficients are the annual probability of mortality in each category. The *trendline equations from top to bottom* are for non-Hispanic whites, non-Hispanic blacks (middle), and non-white Hispanics.

75 years when the Hispanics and non-Hispanic whites diverge from the blacks, the latter demonstrating lower mortality rates. In Figure 3B, this mortality rate is 46% per year between the ages of 98 and 107 for whites. However, this rate is 39% and 40% for blacks and Latinos, respectively. Thus, the "mortality crossover" phenomenon is real. Survival selection is not the only mechanism; inherently long-living phenotypes also exist or can be induced by a positive multimodality (below). *Still, when the annual mortality rate begins to fall to 20, 15, or even 5% in individuals after 110, these cohorts become suspect and certainly form outliers in the trend produced by the bulk of the population.*

Another potential test of longevity data is the female-to-male ratio. *This ratio consistently increases with the age bracket, reaching 9:1 in the 110+ cohort. In the past, the ratio was lower, for example, reaching 1:1 in France in 1816, due to risk during births, postpartum infections, excessive number of pregnancies, status of women in general.* Deviation from the gender composition trend as a function of age presents an anomaly, which is best explicable by the super-longevity group being "contaminated" by the falsified records, where males are represented at 50% or more.

In this context, it is easier to interpret the data for the USA available in the Human Mortality Database. Figure 4 presents the fraction of specific ages in the USA population from 1934 to 2019.

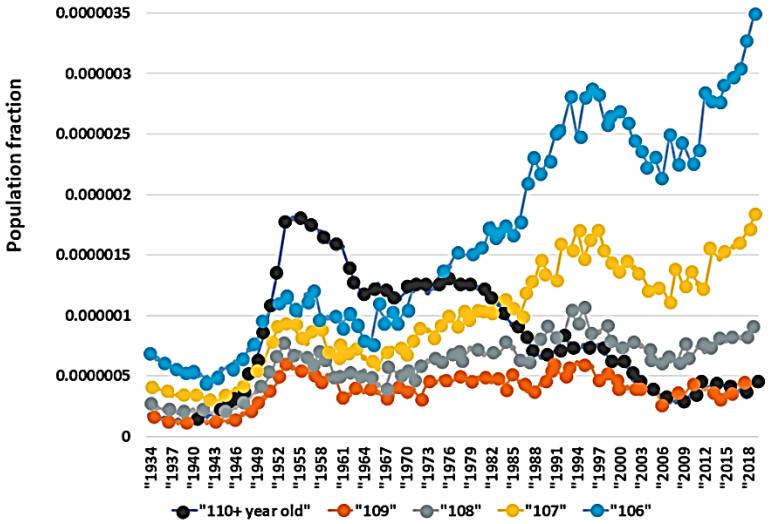

Figure 4: Human Mortality Database Analysis of the USA Population. The number of individuals at the ages indicated on the abscissa was divided by the total population in the respective years. The fractions are displayed. In the year 1955 and in the direction from top to bottom, the ages are: 110+, 106, 107, 108, and 109.

The data in Figure 4 show that *at extremely advanced ages, the lifespan stops responding to the factors that were driving the demographic changes in Figure 1.* The individuals at 109 and 110+ appear with the highest relative frequency in the period between 1943 and 1957, with the subsequent numbers declining. The trend is strongest for 110+, is weaker for 109, and still weaker for 108-year-olds. Table 1 presents the actual lifespans recorded in the NBER. In the cohort of Table 1, the data are more recent, and the birth dates were mostly tracked after the authentication debate. Table 2 presents older data, which is more likely to be "contaminated" by displaced age records.

Table 1: The lifespans recorded in the NBER per 10^6 of the decedents for the period between 1999 and 2018 in the USA. The SUM* (the population of supercentenarians) is adjusted to the total number of decedents (approximately 2.2 x10^6 per year) and accounts for the mortality rate of 0.5 in this age category (see below).

AGES	1999	2003	2004	2005	2011	2014	2015	2016	2017	2018	SUM*
111	8	14	7	11	15	12	11	7	6	6	368.6
112	6	4	5	4	4	1	5	6	2	1	144.4
113	6	10	2		3	3	4	2	3		125.4
114	5	1	2	2	2	1	3		1		64.6
115	2		1	2	1		1		2		34.2
116		3	1	1			1		1		26.6
117	2	1						1			15.2
118						1					3.8

Table 2 presents the data from the same source but accrued between 1959 and 1989. The adjusted sums were computed analogously to those in Table 1.

AGES	"1959 -1969"	"1970 -1979"	"1980 -1989"	SUM *	AGES	"1959 -1969"	"1970 -1979"	"1980 1989"	SUM *
111	**43**	**48**	**85**	**1161.6**	**124**	**2**	**3**	**2**	**46.2**
112	**31**	**30**	**59**	**792**	**125**	**2**	**0**	**3**	**33**
113	**26**	**24**	**47**	**640.2**	**126**	**0**	**2**	**0**	**13.2**
114	**12**	**24**	**37**	**481.8**	**127**	**1**	**3**	**5**	**59.4**
115	**21**	**22**	**25**	**448.8**	**128**	**0**	**0**	**0**	**0**
116	**9**	**18**	**22**	**323.4**	**129**	**0**	**0**	**1**	**6.6**
117	**10**	**8**	**18**	**237.6**	**130**	**0**	**1**	**0**	**6.6**
118	**6**	**6**	**11**	**151.8**	**131**	**0**	**0**	**0**	**0**
119	**2**	**5**	**9**	**105.6**	**132**	**1**	**0**	**0**	**6.6**
120	**6**	**5**	**5**	**105.6**	**133**	**0**	**0**	**0**	**0**
121	**5**	**2**	**2**	**59.4**	**134**	**0**	**0**	**0**	**0**
122	**3**	**1**	**4**	**52.8**	**135**	**1**	**0**	**0**	**6.6**
123	**0**	**3**	**3**	**39.6**	**136**	**0**	**0**	**0**	**0**
					137	**0**	**1**	**0**	**6.6**

The results in Table 1 (more recent data) and Table 2 (historical past) differ in a few substantial aspects. First, in the period between 1959 and 1989, the frequency of ages > 120 is extraordinary. Second, the attrition rates in the values of SUM*, approximating the actual supercentenarian populations, are different between Table 1 and Table 2. The ages of 130 and above are reported in Table 2, with one record being 137! The numbers of supercentenarians in Table 2 exceeded expectations, as predicted by the frequencies in Table 1. All these discrepancies make the extraordinary longevity of Table 2 suspicious, even if similar trends are shown in French data (or Spanish data). The ages above 130 or in the high 120s are most likely the results of clerical errors (NBER consists of > 132 million records) or other artifacts. The ages in the low 120s are reported for the years when the "mortality crossover" effects were stronger (higher birth rates and a higher death rate in younger ages) and when the country was at its historical peak (placebo effect). These results are not totally unrealistic. Another hint that the historical position of a society impacts the maximal lifespan through a placebo effect is the correlation of local peaks and troughs of the supercentenarian fraction as a function of economic booms and recessions (Figure 4). The supercentenarian fractions rise during periods of historical optimism and satisfaction.

Actuarial aging can be defined as an increase in the probability of a final breakdown of a complex system as a function of time.

For reasons certainly worth a discussion, the mathematical expression summarizing the final breakdown in humans, animals, plants, and even machines is known as the Gompertz-Makeham equation:

$$H(T) = a \times \exp(bT) + \lambda \qquad (2)$$

Where H(T) is the probability of dying at the given year, T is the biological age, a is the pre-exponent constant, b is the exponent constant, and λ is the age-independent contribution to mortality.

The form (2) is an oversimplification, as early childhood and centenarian range do not follow this generalization. In fact, the H(T) is < 0.01 for infants in modern societies but used to be much higher. H(T) reaches its minimum of 0.00012 at ~ 10 years, and from that point on, it begins to rise. Puberty brings a sharp rise to H (T), and at 20 years, it is already 0.001. The value of H(T) remains near constant for the entire 17 years between 18 and 35, the period empirically or intuitively called "the prime of life". From the age of about 35, the H(T) curve (also called the "force of mortality" in the terms

of actuarial science) begins its exponential rise, best described by (2). It reaches a value of 0.01 at 59 years and 0.1 at 80 years. After the age of 95, the H(T) course begins to accelerate again, reaching 0.4–0.7 in the 100-year-old. These trends are presented in Figure 5.

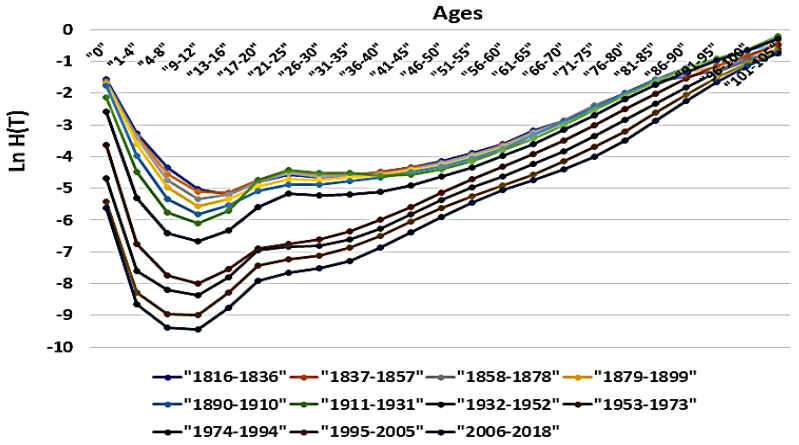

Figure 5: Semilogarithmic plotting of the annual probability of mortality (hazard function H(T)) as a function of age in different historical periods of French society between 1816 and 2016, the data of Human Mortality Database. The 200 years of French history were organized in 20-year intervals (each curve). Within each interval and for all age brackets, the number of decedents was related to the total population, producing age-dependent mortality rates. The bottom curve corresponds to the most recent interval (2006-2018), the top curve corresponds to (1816-1836).

Figure 5 demonstrates that the period from 1816 to 1952 (the top cluster of 7 curves) did not result in as rapid progress as the period between 1953 and 2018 (the bottom cluster of 4 curves). Of note, the tangent of the straight lines formed in the age range 91-105 is higher in modern times and decreases in past historical periods. This sub-trend is consistent with the "crossover" scenarios and selection mechanism since the number of individuals reaching these ages changed by orders of magnitude *and the fitness requirements for reaching older ages were reduced, respectively.*

In Western populations, the value of the constant b is about 0.085, indicating a doubling of mortality risk every 12 years. The constant a is an inherent random risk of failure (see below), and it has a population-averaged value of 0.001. It is interesting to consider the percentage of survivorship in a population that follows the Gompertz-Makeham actuarial statistics.

The survival function can be defined as the fraction of the population with the initial number N_0 still present as N(T) at the age of T.

We write down the connection between the survival function S(T) and the force of mortality H(T):

$$H(T) = - d \ln (S(T))/dt \quad (3)$$

Why is S(T) in the logarithmic form?

The annual change in the number of survivors S(T) in a population produces a metric called f(T), or "probability density of mortality," that masks the real force of mortality.

$$f(T) = - dS(T)/dT \quad (4)$$

To obtain the true value of H(T), one needs to account for the shrinking number of survivors compared to N_0.

The corrected and uncorrected values relate to:

$$H(T) = f(T)/(1 – F(T)) \quad (5)$$

Where F(T) is the cumulative fraction of all individuals that died by the age of T, f(T) is the uncorrected value, and H(T) is the corrected value.

With 1 - F(T) = S(T), which is the population of the survivors, one obtains the form (3). The fraction of survivors by age T thus becomes:

$$\text{Ln } S(T) = \int [- \lambda - a \text{ x } \exp (bT)] \, dT \quad (6)$$

Integration of the logarithmic form and elementary transformations gives:

$$S(T) = S(0) \exp (- \lambda T – (a/b) \exp (bT)) \quad (7)$$

Where S(T) is the number of survivors in the population, S(0) is the initial number, and T is the time since birth. *The equation (7) shows that a hypothetical non-aging population will still decline.*

$$S(T) = S(0) \exp (- \lambda T) \quad (8)$$

For a hypothetical population with $a > 0$, but $b = 0$, λ and a would combine in (2):

$$H(T) = a + l \quad (9)$$

The number of survivors will also decline under the Weibull law.

$$S(T) = S(0) \exp (- (\lambda + a) T) \quad (10)$$

The logarithm of both parts leads to a linear equation:

$$\text{Ln } S (T2) – \text{Ln } S (T1) = - (\lambda + a) (T2 – T1) \quad (11)$$

A non-aging population (with a constant annual breakdown risk, and no increase with time) will follow the equation (11). The survival fraction in this scenario declines like the nuclei in radioactive decay, with a constant annual fraction. The plot will be a downward-directed straight line with a constant tangent. An aging population will show a nonlinear plot downward-directed from the straight line in these coordinates; a population of aging-reversing organisms will produce an upward-deviating plot. With this understanding, we explored the USA, Japanese, and French data to estimate if aging is a constant presence in human life or whether there are periods when it is absent (or at least it seems so based on the plotting procedure). The plotting also allows us to estimate the expected maximal lifespan for a given historical period. When ln S = 0, this means only 1 individual is still alive in the population, following the exponential decay law (11). If there is a linear fit in the form Ln N = B [Age] + C, where N is the number of survivors at a given age, B [Age] = - C is the condition of reaching a maximal lifespan. In analytical form,

$$N(T + DELTA) = N(T) \times (\lambda + a)^{DELTA} \quad (12)$$

Where DELTA is the time interval required to bring the population numbers from N(T) to N(T + DELTA) = 1. The sum T + DELTA represents the lifespan estimate. Figure 6 presents the analysis, including changes in the lifespan estimates for the respective societies in different historical periods.

Figure 6 shows that in three different societies, the effective maximal *lifespan is a dynamic characteristic that depends on the country's size and historical context* (USA > Japan > France). It generally varies in the range between 111 and 121 years, and the higher numbers for the USA in 1943–1993 are likely artifacts due to imperfect birth records prior to the reforms (Newman et al.). The currently observed fraction of nonagenarians and centenarians strongly lags the theoretical fraction based on the survival function (Figure 1). *This disconnect is due to the rapid pace of progress and social changes.* With the Earth's population of 9 billion and the decay coefficient (a + λ) equaling 0.5, the maximal observed lifespan may grow to 133.2 years (assuming all factors act as today).

Figure 6: Semilogarithmic plots of the population numbers N as a function of age in the USA (6A), Japan (6B), and France (6C). The data are fitted by a linear function, The order corresponds to the order of the fitted lines, from top (more recent ranges) to bottom (deeper in the past). The maximal age existing in the given population at the given historical period can be found from the ratio of the vertical intercept to the tangent. The maximal ages are summarized in the table. The tangent values in the legend relate to the numbered equations in the figure and to the respective linear plots. The more recent intervals correspond to the upper lines and to the lower equation numbers. The analyzed time intervals are shown below each abscissa.

USA			Japan			France		
Period	$\lambda + a$	Age	Period	$\lambda + a$	Age	Period	$\lambda + a$	Age
1933-1943	0.4059	122.48	1947-1956	0.416	114.01	1816-1836	0.8123	108.900
1944-1953	0.3718	125.16	1957-1966	0.537	111.75	1858-1878	0.8546	108.918
1954-1963	0.3665	126.64	1967-1976	0.793	110.77	1890-1910	0.8226	109.848
1964-1973	0.3859	125.84	1977-1986	0.724	112.20	1932-1952	0.5877	114.349
1974-1983	0.4277	125.03	1987-1996	0.670	114.79	1974-1994	0.6778	115.447
1984-1993	0.4617	124.55	1997-2006	0.663	117.19	2006-2018	0.6364	118.68
1994-2003	0.5441	122.29	2007-2016	0.625	119.92			
2004-2013	0.5966	120.79	2017-2021	0.587	121.84			
2014-2020	0.619	120.61						

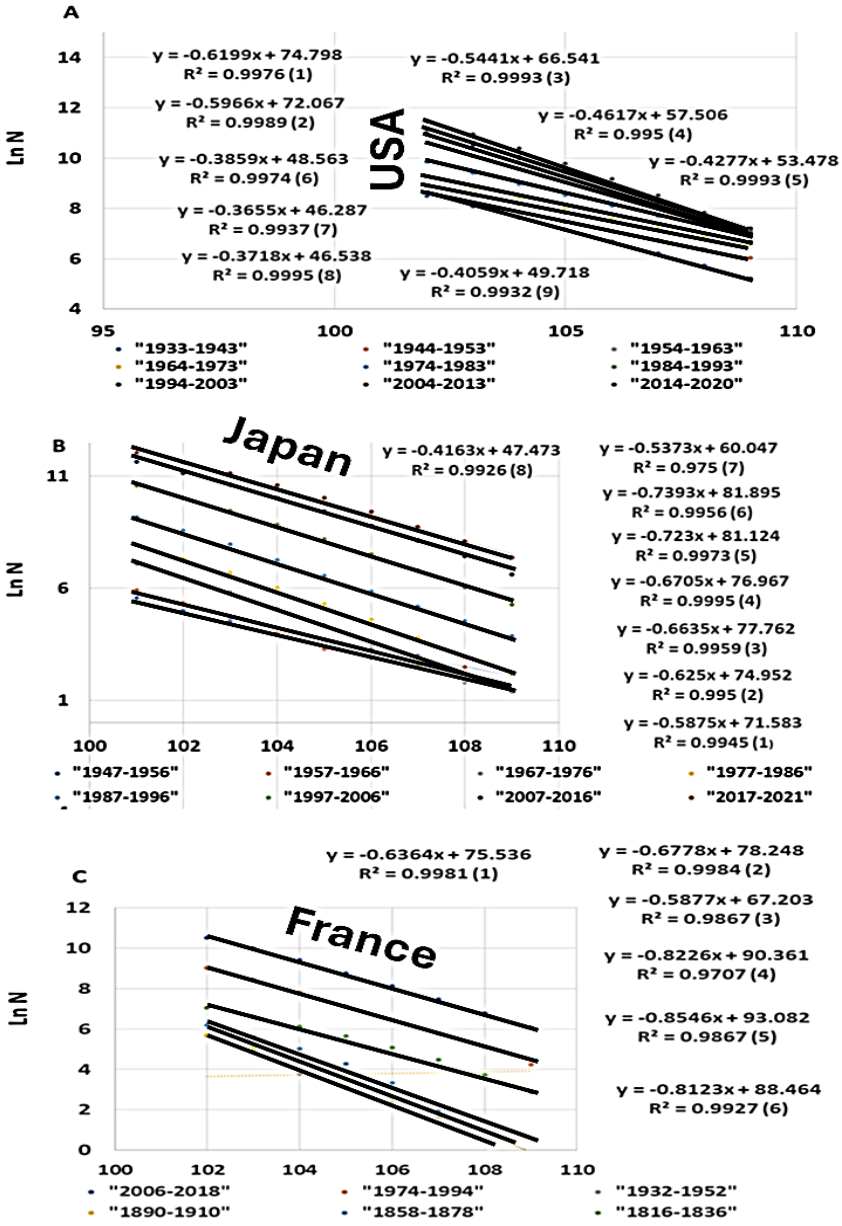
A
USA
Ln N
y = -0.6199x + 74.798
R² = 0.9976 (1)
y = -0.5966x + 72.067
R² = 0.9989 (2)
y = -0.3859x + 48.563
R² = 0.9974 (6)
y = -0.3655x + 46.287
R² = 0.9937 (7)
y = -0.3718x + 46.538
R² = 0.9995 (8)
y = -0.5441x + 66.541
R² = 0.9993 (3)
y = -0.4617x + 57.506
R² = 0.995 (4)
y = -0.4277x + 53.478
R² = 0.9993 (5)
y = -0.4059x + 49.718
R² = 0.9932 (9)
"1933-1943"
"1944-1953"
"1954-1963"
"1964-1973"
"1974-1983"
"1984-1993"
"1994-2003"
"2004-2013"
"2014-2020"
B
Japan
Ln N
y = -0.4163x + 47.473
R² = 0.9926 (8)
y = -0.5373x + 60.047
R² = 0.975 (7)
y = -0.7393x + 81.895
R² = 0.9956 (6)
y = -0.723x + 81.124
R² = 0.9973 (5)
y = -0.6705x + 76.967
R² = 0.9995 (4)
y = -0.6635x + 77.762
R² = 0.9959 (3)
y = -0.625x + 74.952
R² = 0.995 (2)
y = -0.5875x + 71.583
R² = 0.9945 (1)
"1947-1956"
"1957-1966"
"1967-1976"
"1977-1986"
"1987-1996"
"1997-2006"
"2007-2016"
"2017-2021"
C
France
Ln N
y = -0.6364x + 75.536
R² = 0.9981 (1)
y = -0.6778x + 78.248
R² = 0.9984 (2)
y = -0.5877x + 67.203
R² = 0.9867 (3)
y = -0.8226x + 90.361
R² = 0.9707 (4)
y = -0.8546x + 93.082
R² = 0.9867 (5)
y = -0.8123x + 88.464
R² = 0.9927 (6)
"2006-2018"
"1974-1994"
"1932-1952"
"1890-1910"
"1858-1878"
"1816-1836"

3. Does human senescence proceed at a variable or constant rate?

Figure 6 shows that mortality follows linearity in the log plot for ages > 100 years. Does that mean the cessation of aging after a critical parameter of frailty is reached? And what is the meaning of the apparently decreased aging rate between 18 and 35 years in Figure 5? If such a fundamental process can be switched on and off or modified to accelerate and decelerate, that would mean a powerful aging program, perhaps resembling what is observed in the Pacific salmon (Gems et al.). Such programmed aging is switched off in salmon rather easily, and it would be tempting to discover a similar program in humans.

We directly tested the hypothesis that the human aging rate is variable over a lifetime. The tool of verification was a database of the National Alzheimer's Coordinating Center (https://naccdata.org/). The NACC data represents a longitudinal dataset with dated patient visits. Not only patients but also relatives are included in the study and participate in cognitive testing, and the clinician's assessment of health status. All diagnoses are recorded in a time-dependent manner. The individuals leave the observation when they quit, or when they die between the scheduled visits. In this setting, we traced the development of age-related pathologies and the length of observation as a function of baseline age. We suspected that the early adulthood bends of Figure 5 and the late-life Weibull dependence in Figures 5 and 6 are evidence that the aging rate in humans can change its pace analogously to what is observed in semelparous fish.

The analysis shows that the NACC population is variable in terms of individual aging rates. In the individuals with 1 year left of follow-up (life expectancy), the rate of dementia at baseline reached 40%, polypharmacy was 3.4 prescription pharmaceuticals per person, and cardiovascular disease was at 0.3 conditions per person. The mortality rate in this group reached 28% after only one year of observation. By contrast, the individuals in the slow aging group with follow-up of 13 years were at the age of 91 and demonstrated baseline dementia of 3% (at 78 years), final dementia of 25% at 91 years*, and a final mortality rate of 8% after 13 years of observation!* The difference between the fast- and slowly aging strata is dramatic, corresponding to decades of life expectancy variation between the extreme cohorts. *All baseline metrics are inversely correlated with the residual life expectancy, and this simple linear relationship makes them aging markers*. If there is a program decelerating the aging rate after it reaches an already dangerously high value in the elderly, the rate of disease, polypharmacy,

and dementia acquisition will fall in these age brackets. But the marker derivatives will continue to rise or remain the same if there is no deceleration stage. Figure 7 resolves the question.

The results of Figure 7 demonstrate an accelerating trend (increasing time derivatives) in the value of senescence markers. The p-values of the T-test between the cardiovascular morbidity derivative and dementia in the 90–94 and >95 groups are significant. These results rule out the deceleration of aging in the elderly. The linearity of the log plot in Figure 5, which is typically used as an argument for such deceleration (Weibull statistics of extinction), can be explained alternatively. *For example, at extreme ages, genetic robustness becomes the dominant factor, and the mortality rates at the edge of distribution increase due to aging but decrease in the same proportion due to the outstanding robustness of the most viable members of the population*. The mutual compensation of two factors creates the illusion of arrested senescence in the oldest (see Wrigley-Field).

Another phenomenon that may suggest variable or programmed rates of human aging is the bent shape of the annual mortality semi-logarithmic plot (Figure 5) between the ages 15–35, which otherwise must be linear in that range, similarly to the range 35–100. The leftmost region (0–10 years) can be rationalized within the framework of reliability theory. The hazard function H(T) of the Gompertz distribution resembles the bathtub reliability function for non-animated items, such as a vehicle tire. The total probability of failure for a vehicle tire passes through a minimum of a couple of years after installation, and the shape of the plot vs. time resembles a cross-section of a bathtub. The early failure reflects the consequences of production defects that manifest upon stressing the item. This component becomes less likely with the passage of time since larger defects tend to manifest earlier. The second component is random. A combination of fluctuations and accidents can lead to a tire puncture or a crack in the metal frame. This component is not time dependent. The third component increases with time and is called “wear-out failure." It reflects tiredness, corrosion of metal parts, accumulation of microdefects, and oxidation in the organic parts of the tire. One can draw parallels with the H(T) profile for humans. Indeed, the owners of old computers or cars may have noticed that maintenance becomes progressively more expensive as the item ages. With relatively high child mortality risk, a minimum in the intervening years, and an exponential rise of the hazard function in the later years, our fragility also follows the Bathtub profile. These comparisons between aging humans, computers, and cats became the basis for the reliability theory of aging

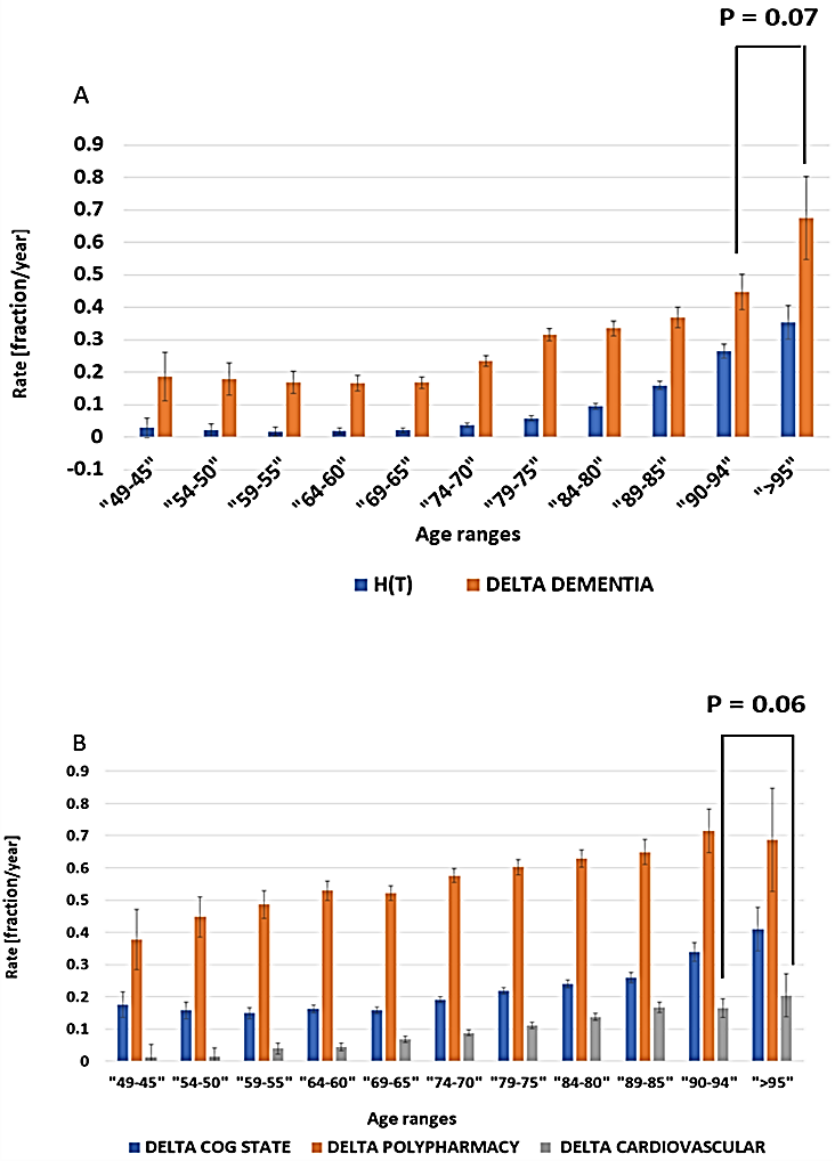

Figure 7: Time-derivatives of aging markers as a function of age. The NACC dataset (42,000 patients) was sorted by follow-up, and the zero-follow-up cohort was discarded. The patients with dementia at baseline were also discarded. The

remaining 21300 patients were organized in intervals of 5 years by age. For each patient, the difference between the final and baseline values of the senescence markers (Figure 7) was related to the follow-up interval. The average of these derivatives for each age group was computed and plotted. The order of the markers in each age interval as shown in the legend (in the series of three bars per each age-range, the left is delta cognitive state, the central is delta polypharmacy, the right is delta cardiovascular disease) . Variation was assessed by CI95 confidence intervals. The differences between the parameters in the respective cohorts were assessed by a one-tail equal variance t-test.

(Gavrilov et al.); however, simplistic consideration of living organisms as machines with original and acquired defects does not correctly reflect the essence of biological aging. The process of regeneration and remodeling in living organisms can be sweeping and, in some cases, total. Perhaps failures occur when the living systems do not sufficiently renovate the critical parts. To see that this is the case, one must review the opposite situations, when total repair and rejuvenation take place (below). Also, aging and frailty do not always align. A 10-year-old child is older than a 1-month-old infant, yet is also more developed, with stronger immunity, more stable homeostasis, better coordinated organ systems, and a more developed brain orchestrating most of the other organismal functions. This superposition of aging and development reduces observed mortality despite continuous aging. Only in the post-puberty period, when development is complete, does the net effect of aging begin to impact mortality statistics. But how to explain the sharp rise in mortality during puberty and the plateau between 20 and 35 (Figure 5)? To address this question, we accessed the latest Multiple Causes of Death (MCD) data from the National Bureau of Economic Research (NBER, 2018). Figure 8 presents the results.

To our surprise, the mortality in the violence/accident medical codes (S, T*, U*, V*, W*, X*, Y*, Z*) was extraordinarily high in US society, reaching 15% of the total.* The peak in this distribution falls in young adulthood (16-30) and roughly matches the peak of testosterone production. The “bathtub” profile remains in Figure 8 for aging-related causes. Another surprising observation is that the maximum in relative cancer mortality is falling to 70 years, and sharply declines in the oldest old. The relative mortalities from respiratory, digestive, renal, and mental disorders also follow the extremum and decline in the oldest old. Yet cardiovascular, neurological, and endocrine diseases form an increasing share of total mortality as a function of age. Figure 9 confirms the mortality data from the prevalence study in the living patients of NACC.

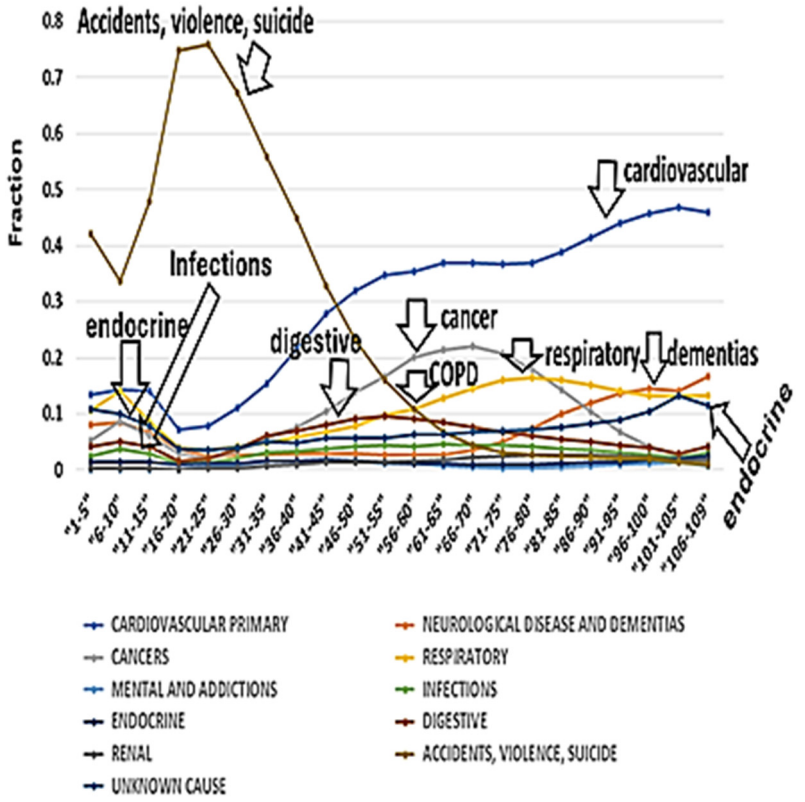

Figure 8: Fractions of all-cause mortality by cause as a function of age. The 10^6 decedents registered in NBER were stratified into 5-year intervals by age. In each interval, the number of decedents attributed to a particular ICD-10 medical code was related to the total number (all codes). In terms of ICD-10 codes, cardiovascular disease is I*, cancers C*, neurological G* and F03*, respiratory/COPD J*, mental and addictions F*, infections A* and B*, endocrine E*, digestive K*, renal N*, accidents, violence, and suicide are S*, T*, U*, V*, W*, X*, Y*, and Z*. The curves corresponding to the descriptions are located right under the titles and are labeled by tags accompanied by hollow arrows touching each respective curve.